MODELING OF PAVEMENT ROUGHNESS UTILIZING ARTIFICIAL NEURAL NETWORK APPROACH FOR LAOS NATIONAL ROAD NETWORK

Mohamed GHARIEB[1], Takafumi NISHIKAWA[1*],
Shozo NAKAMURA[1], Khampaseuth THEPVONGSA[2]

[1]*Graduate School of Engineering, Nagasaki University, 1-14 Bunkyo-machi, Nagasaki 852-8521, Japan*
[2]*Faculty of Engineering, National University of Laos, Lao-Thai Road, Sokpaluang Village, Sisatanak District, Vientiane Capital, Laos*

Abstract. The International Roughness Index (IRI) has become the reference scale for assessing pavement roughness in many highway agencies worldwide. This research aims to develop two Artificial Neural Network (ANN) models for Double Bituminous Surface Treatment (DBST) and Asphalt Concrete (AC) pavement sections using Laos Pavement Management System (PMS) database for National Road Network (NRN). The final database consisted of 269 and 122 observations covering 1850 km of DBST NRN and 718 km of AC NRN, respectively. The proposed models predict IRI as a function of pavement age and Cumulative Equivalent Single-Axle Load (CESAL). The obtained data were randomly divided into training (70%), validation (15%), and testing (15%) datasets. The statistical evaluation results of the training dataset reveal that both ANN models (DBST and AC) have good prediction ability with high values of coefficient of determination ($R^2 = 0.96$ and 0.94) and low values of Mean Absolute Error (MAE = 0.23 and 0.19) and Mean Squared Percentage Error (RMSPE = 7.03 and 9.98). Eventually, the goodness of fit of the proposed ANN models was compared with the Multiple Linear Regression (MLR) models previously developed under the same conditions. The results show that ANN models yielded higher prediction accuracy than MLR models.

Keywords: International Roughness Index (IRI), Laos pavement management system (PMS), artificial neural network (ANN), backpropagation algorithm, double bituminous surface treatment (DBST), asphalt concrete (AC), pavement age, cumulative equivalent single-axle load (CESAL), pavement performance model.

Introduction

Laos is a landlocked country located in the Indochina peninsula which shares borders with five countries: China, Vietnam, Thailand, Myanmar, and Cambodia. Its unique location allows it to transfer to land-linked countries that connect its neighbors through its National Road Network (NRN). Over the last three decades, Laos has seen essential progress in improving the road infrastructure, where the road network length has grown from only 14,000 km in 1990 to be 58,255 km in 2020 (Asian Infrastructure Investment Bank [AIIB], 2009; Laos Ministry of Public Works and Transport, 2020). The Laos road network is divided into six classes: (i) National Roads (NRs); (ii) Provincial Roads (PRs); (iii) District Roads (DRs); (iv) Urban Roads (URs); (v) Rural Roads (RRs); and (vi) Special Roads (SRs). As shown in Table 1, the greatest share of the total length of the network is dominated by RRs (43.32%), followed by PRs (14.86%), NRs (13.22%), and the lasting 28.60% are DRs, URs, and SRs (Laos Ministry of Public Works and Transport, 2018, 2020).

Laos paved roads are categorized according to their structural properties into three groups: Double Bituminous Surface Treatment (DBST), Asphalt Concrete (AC), and Cement Concrete (CC). NRs involve roughly 7700 km of the road network (as illustrated in Figure 1), the superiority of which (85.84%) have a paved surface, while gravel and earth sections comprise only 10.70% and 3.46% of them, respectively. Most NRs' paved sections are DBST (71.64%), while AC and CC cover just 13.00% and 1.20% of them, respectively (Laos Ministry of Public Works and Transport, 2020).

Corresponding author. E-mail: nishikawa@nagasaki-u.ac.jp

Table 1. Basic statistics of Laos road network 2020 (Laos Ministry of Public Works and Transport, 2018, 2020)

Type of Road		DBST (km)	Asphalt (km)	Concrete (km)	Gravel (km)	Earth (km)	Total	
							Length (km)	Proportion (%)
National Roads		5516.91	1001.03	92.43	823.65	266.55	7700.57	13.22
Provincial Roads		2067.41	64.70	91.53	5044.29	1389.48	8657.41	14.86
District Roads		720.39	0.00	67.83	4438.95	1947.54	7174.70	12.32
Urban Roads		1341.19	134.17	292.98	1457.11	807.18	4032.64	6.92
Rural Roads		756.28	4.00	46.93	10,877.94	13,549.13	25,234.27	43.32
Special Roads		350.20	11.53	57.71	1234.75	3800.69	5454.88	9.36
Total	Length (km)	10,752.38	1215.43	649.40	23,876.69	21,760.57	58,254.48	100.00
	Proportion (%)	18.46	2.09	1.11	40.99	37.35	100.00	

Pavement performance prediction models are an essential component in any Pavement Management System (PMS) because they play a crucial role in forecasting pavement performance in the future, estimating maintenance and rehabilitation needs, and setting priorities among projects under restricted funds (Al-Mansour & Al-Swailem, 1999).

The World Bank evolved Laos PMS in 2004 to include the NRN (Japan International Cooperation Agency [JICA] & Mitsubishi Research Institute, 2013). Laos PMS employs the Highway Development and Management Model (HDM-4) as an analysis engine to set roads' short- and medium-term maintenance strategies (Gharieb & Nishikawa, 2021).

Pavement deteriorates under the combined effect of different factors such as traffic loads and environmental condition (George et al., 1989; Surendrakumar et al., 2013). A considerable number of variables need to be taken into consideration for predicting pavement performance. Ideally, these variables involve pavement age, material properties, traffic loads, subgrade properties, and environmental factors (Gupta et al., 2011; Owusu-Ababio, 2002).

Transportation agencies utilize several indices to depict pavement condition, such as the Present Serviceability Rating (PSR), Pavement Condition Index (PCI), International Roughness Index (IRI), and the Present Serviceability Index (PSI) (Shahnazari et al., 2012). All these indices transform pavement distresses into a more practical index (Smith & Ram, 2016). The roughness of pavement is one of the most interesting characteristics that can be measured from roads because the roughness of a pavement surface can affect ride quality, driving safety, and vehicle operating cost (Zang et al., 2018). Rough surface considerably impacts vehicle speed, fuel consumption, tire wear and increases maintenance costs of road surfaces (Abulizi et al., 2016).

In 1986, IRI was initially introduced in a research effort driven by the World Bank, which aimed to establish a global and transportable index to quantify pavement roughness (Sayers et al., 1986a, 1986b). IRI is calculated based on the dynamic response of a mathematical model called "quarter-car". The IRI is defined as "the accumulated suspension vertical motion divided by the distance traveled as obtained from a mathematical model of a simulated quarter-car traversing a measured profile at 80 km/h" (ARA, 2001). The IRI is usually measured in meters per kilometer or inches per mile (Múčka, 2017). At present, due to its stability over time and transferability over the world, it has become the most widely employed pavement index, not only for roughness assessment, with examples in both developed countries (Pérez-Acebo et al., 2021; Sidess et al., 2020; Yamany et al., 2021; Yamany & Abraham, 2021) and developing countries (Albuquerque & Núñez, 2011; Nguyen et al., 2019; Obunguta & Matsushima, 2020; Olowosulu et al., 2021; Pérez-Acebo et al., 2019).

In Laos, road maintenance strategy is mainly based on assessing pavement roughness evaluated in terms of the IRI. The Laos Public Works and Transport Institute (PTI) collects the IRI data for NRN utilizing the Dynamic Response Intelligent Monitoring System (DRIMS) provided to the Laos government as technical support by Nagasaki University in a JICA technical cooperation project (Japan International Cooperation Agency (JICA) & Mitsubishi Research Institute, 2013). DRIMS has been developed to be a low-cost solution for road authorities to monitor and evaluate their road network. This made roughness data in IRI a simple, convenient, and inexpensive indicator for monitoring and assessing changes in different pavement surfaces (Gharieb & Nishikawa, 2021).

DRIMS comprises both hardware and software. Figure 2a illustrates the four main components of DRIMS hardware: (i) laptop; (ii) data acquisition module; (iii) accelerometer; and (iv) GPS logger, which all are connected via cables. As shown in Figures 2b and 2c, The DRIMS software includes two kinds of applications that are uniquely developed (Asakawa et al., 2012; Fujino et al., 2005): an application for data acquisition and calibration (Figure 2b) and an application to carry out the analysis (Figure 2c). By utilizing these two applications, the required data were measured and analyzed then the IRI value was calculated every 100 m interval over the traveled distance (Douangphachanh & Oneyama, 2014).
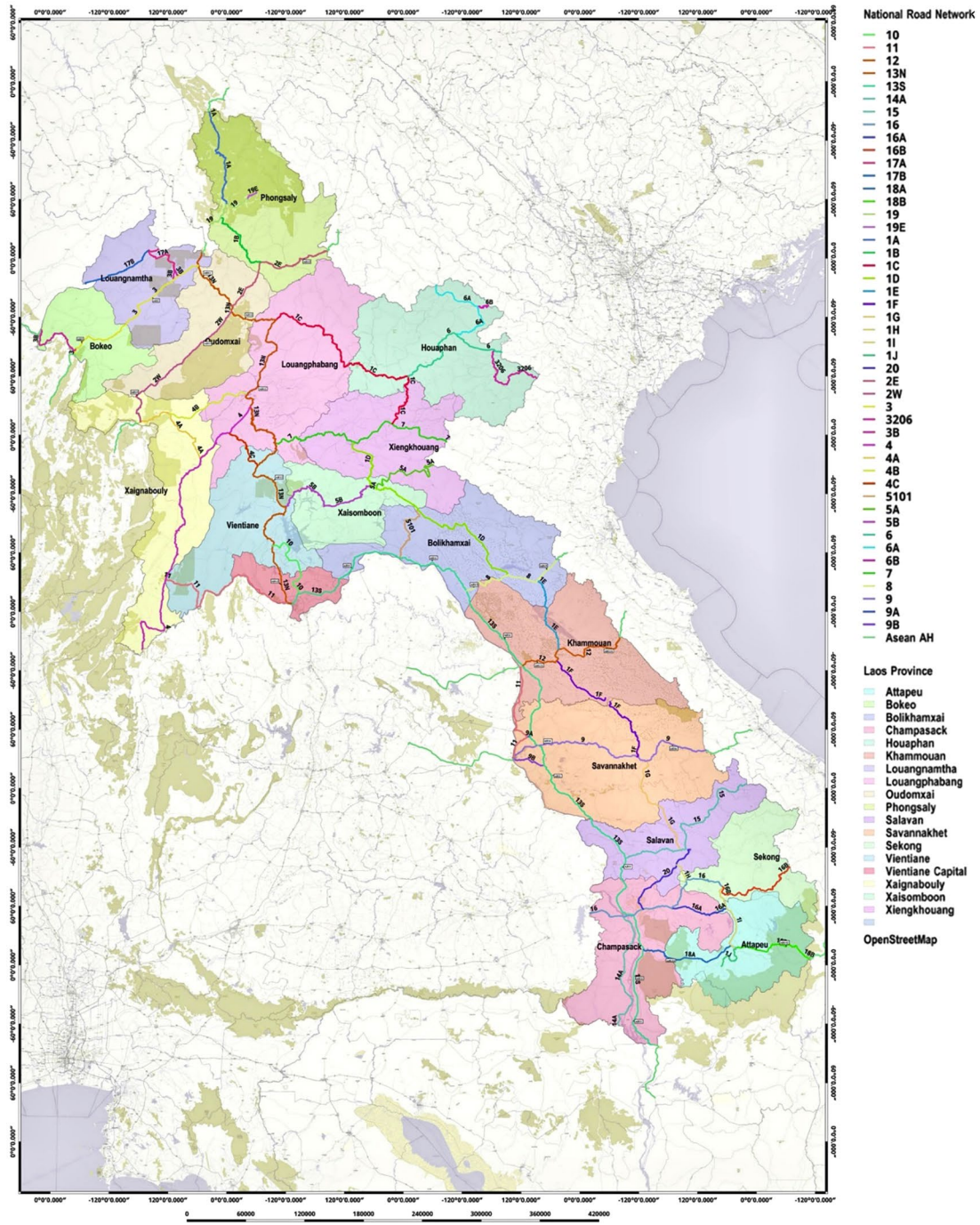
Figure 1. Laos National Road Network (Laos Ministry of Public Works and Transport, 2020)

a)   b)   c)
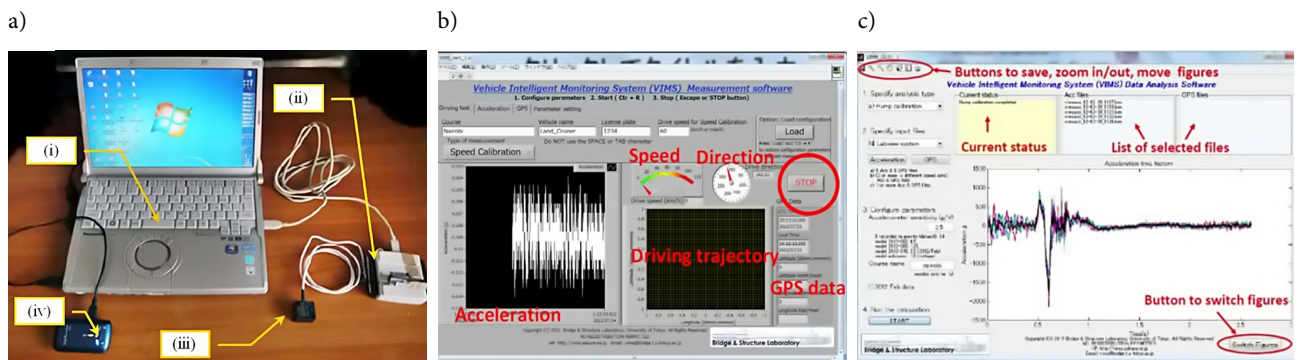

Figure 2. DRIMS: a – Hardware components; b – Data collection and calibration application; c – Data analysis application
(Asakawa et al., 2012; Fujino et al., 2005)

Laos PMS uses default HDM-4 pavement deterioration models without calibration to predict the IRI, which leads to an enormous error between measured and predicted IRI values. Thus, developing an accurate IRI prediction model is necessary based on Laos's local conditions to operate PMS precisely.

There are different types of pavement deterioration models in the literature, which are classified depending on the authors. For instance, the pavement management guide (American Association of State Highway and Transportation Officials [AASHTO], 2012) grouped them into deterministic, probabilistic, Bayesian, and subjective (or expert-based) models. Similarly, Uddin (2006) classified the prediction models into deterministic (mainly based on regression analysis), probabilistic (including mainly the Markovian and Bayesian models), and Artificial Neural Network (ANN) models. Additionally, Justo-Silva et al. (2021) classified them into deterministic, probabilistic, and hybrid (including Fuzzy Logic, ANN, and Neuro-fuzzy). Nevertheless, the deterministic and the probabilistic models are the most widely used and they are recognized as the basic groups (Abaza, 2016, 2018).

Modeling via traditional regression methods is very complicated and requires predefinition of the form of the regression equation. So, over the last two decades, the ANN has attracted pavement experts' interest in analyzing prediction problems involving very complex relationships among variables (Kırbaş & Karaşahin, 2016). Lately, there has been a wide variety of studies with the specific objective of applying the ANN approach in modeling pavement roughness (Abd El-Hakim & El-Badawy, 2013; Abdelaziz et al., 2020; Choi et al., 2004; Chou & Pellinen, 2005; Georgiou et al., 2018; Hossain et al., 2020; Kaloop et al., 2020; La Torre et al., 1998; Lin et al., 2003; Mazari & Rodriguez, 2016; Teomete et al., 2004; Ziari et al., 2015). Most of these models were developed using the Long-Term Pavement Performance (LTPP) database, whereas others were derived based on direct field measurements or the regional agency PMS database. Table 2 summed up some of the previous studies' results that applied different techniques in modeling IRI.

The literature review of the existing IRI prediction models for different pavement types revealed that:
- ANN models show good performance in predicting and determining pavement roughness condition over the years.
- Despite the advantages of the ANN technique, some authors regard the ANN models as a "black box" as it is impossible to know the exact influence of each factor (variable) (Pérez-Acebo et al., 2020; Sollazzo et al., 2017).
- Most of these models were developed based on a localized database, preventing them from being used globally.
- Variables such as traffic loads, pavement age, pavement distresses, environmental conditions, and structural strength significantly affect pavement roughness deterioration.

- Relatively few studies have been conducted to predict the IRI of DBST pavement sections, most of which were about CC and AC pavement.

This research, hence, aims to develop two indigenous models for predicting the IRI of DBST and AC pavement sections for Laos NRN utilizing an ANN technique and compare its accuracy with the Multiple Linear Regression (MLR) models that were previously developed under the same conditions. The main objective of the developed models is to provide Laos PMS with precise IRI prediction models to assist the accountable authorities in making consistent maintenance decisions to deteriorated pavement sections.

1. Methodology

To fulfill the research objective, the methodology followed in this study commenced by reviewing the relevant literature. Then, the MLR models were defined as developed previously. After that, ANN approach was applied to develop the proposed models. Basic statistical analyses were conducted to evaluate and clarify the proposed models' sensitivity. Finally, the proposed ANN models were compared statistically with the MLR models for DBST and AC pavement sections. The research methodology is summed up in Figure 3.

1.1. Multiple linear regression models

The modeling was based on the Laos PMS database of the NRN. The original database included measurements on 214 and 36 pavement sections covered DBST and AC paved NRN over 14 years, starting from 2001 till 2015. After data screening, the valid number of sections and observations were declined, as illustrated in Table 3 (Gharieb & Nishikawa, 2021).

MLR models were developed utilizing the valid number of observations, including 269 observations from 83 sections covering a total length of 1849.26 km of DBST NRs and 122 observations from 29 sections covering a total length of 718.55 km of AC NRs. Gharieb and Nishikawa (2021) reported efforts regarding data gathering, processing, and variables' calculation. MLR models are defined as shown in Eqns (1)–(2). In addition, Table 4 illustrates the description of models' variables.

$$\text{IRI}_{\text{DBST}} = 3.006 + 0.259 \text{ age} + 0.038 \text{ CESAL}; \quad (1)$$

$$\text{IRI}_{\text{AC}} = 1.782 + 0.203 \text{ age} + 0.123 \text{ YESAL}. \quad (2)$$

It was noticed that the YESAL was used in the IRI_{AC} model (Eqn (2)) instead of CESAL, contrary to what is expected, as was done in the IRI_{DBST} model (Eqn (1)) to avoid multicollinearity among independent variables (Gharieb & Nishikawa, 2021). Multicollinearity emerges when independent variables that are strongly correlated exist in the model (Alin, 2010). Table 5 illustrates the correlation between variables utilizing the Pearson correlation coefficient.

Table 2. Summary of literature IRI prediction models

Authors, year	Pavement type	Source of data	Modeling*	Independent variables*	Model performance
La Torre et al. (1998)	AC pavement	LTPP GPS-1 database	ANN	ACTH, ACEM, UTH, UEM, SEM, FI, AP, ESAL, AGE_0, IRI_0	RMSE = 0.113, N = *144*
Lin et al. (2003)	NA	Direct field measurement, Taiwan	ANN	RL, LRUT, RRUT, AC, CR, D/P, P, MPH, SPH, BLD, COR, STR, MMH, SMH	R^2 = 0.84, RMS = 0.068, N = *100*
Choi et al. (2004)	AC on granular base	LTPP GPS-1 database	ANN	P_{200}, ACTH, ASC, SN, CESAL	r = 0.87, MSE = 0.025, N = 92
			MLR		r = 0.46, MSE = 0.278, N = 117
Teomete et al. (2004)	Jointed Portland Cement Concrete (JPCC)	LTPP database	ANN	IRI_0, AGE, TFAULT, TCLS, TCMS, TCHS, ESAL	R^2 = 0.84, N = 5045
Chou and Pellinen (2005)	Portland Cement Concrete (PCC)	Indian pavement management system database	ANN	IRI_0, AGE, FI, AP, F/T, ESAL	R^2 = 0.98, RMSE = 0.074, N = 90
	Asphalt overlay on concrete pavement				R^2 = 0.88, RMSE = 0.124, N = 1080
	Hot-Mix Asphalt (HMA)				R^2 = 0.90, RMSE = 0.121, N = 640
Abd El-Hakim and El-Badawy (2013)	Jointed Plain Concrete Pavement (JPCP)	LTPP database	ANN	IRI_0, AGE, TC, SPALL, P, TFAULT, FI, P_{200}	R^2 = 0.83, S_e/S_y = 0.414, N = 184
Ziari et al. (2015)	AC over granular base	LTPP database	ANN	AGE, AAP, AAT, AAFI, AADT, AADTT, ESAL, STH, PTH	R^2 = 0.90, RMSE = 0.09, MAPE = 5.54, N = 205
			GMDH		R^2 = 0.63, RMSE = 0.405, MAPE = 28.62, N = 205
Mazari and Rodriguez (2016)	AC over unbound granular layers	LTPP database	Hybrid GEP-ANN	SN, AGE, CESAL	R^2 = 0.99, RMSE = 0.049, N = 95
Abdelaziz et al. (2020)	AC overlay	LTPP database for six sections; GPS-1, 2, 6; SPS-1, 3, 5	ANN	IRI_0, AGE, FC, TC, SDRUT	R^2 = 0.75, N = 2439
			MLR		R^2 = 0.57, SE = 0.325 N = 2439
Georgiou et al. (2018)	AC pavement	Direct field measurement, Greece	ANN	CR, RUT, PH	R^2 = 0.96, MAE = 6.9%, RMSPE = 8.3%
			SVM		R^2 = 0.93, MAE = 7.7%, RMSPE = 8.9%
Hossain et al. (2020)	Rigid pavement	LTPP database	ANN	AAT, AAFI, AAMiH, AAMaH, AAP, AADT, AADTT	RMSE = 0.01, MAPE = 0.01
Kaloop et al. (2020)	JPCP	LTPP GPS-3 database	ANN	IRI_0, FI, TFAULT	r = 0.80, MAE = 0.37, RMSE = 0.49, N = 184
			WOPELM		r = 0.92, MAE = 0.23, RMSE = 0.24, N = 184
Terzi (2013)	Flexible Pavement	LTPP-IMS Database	ANFIS	AGE, SN, CESAL	R^2 = 0.97
Pérez-Acebo et al. (2021)	Semi-rigid pavement	PMS of the regional government of Biscay	MLR	R.Age, TotVeh, TotBit, TotH. Veh, BASE, Bthick, SURF	R^2 = 0.645, SEE = 0.341 N = 81
Nguyen et al. (2019)	AC pavement	2811 Samples as a case study in the North of Vietnam	PSOANFIS	Road Length, Analysis Area, Summed Cracks, Maximum Depth of Rut, Average Depth of Rut	R = 0.888, RMSE = 0.145
			GANFIS		R = 0.872, RMSE = 0.155
			FAANFIS		R = 0.849, RMSE = 0.170
			ANN		R = 0.804, RMSE = 0.186

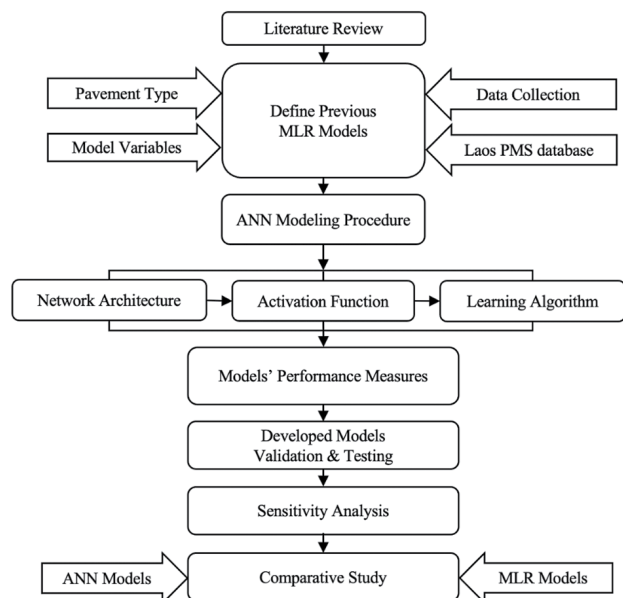*Note*: * All abbreviation definitions are provided in Table A1, Appendix.

Figure 3. Flow chart of the research methodology

Table 3. Summary of the number of sections and observations in each surface-type group

Surface type	Total No. of sections	Total No. of observations	Valid No. of sections	Valid No. of observations
DBST	214	997	83	269
AC	36	184	29	122

Table 4. MLR model variables' description

Variable	Description	Unit
IRI_{DBST}	The predicted value of the IRI for DBST pavement sections	m/km
IRI_{AC}	The predicted value of the IRI for AC pavement sections	m/km
Age	Pavement age since the last overlay to the day of the IRI reading	years
CESAL	The cumulative number of equivalent single axle loads that pavement experienced from the last overlay to the day of the IRI reading	10^4 axles/lane
YESAL	The average cumulative equivalent single axle loads that pavement experienced from the last overlay to the day of the IRI reading (CESAL/Age)	10^4 axles/lane

As seen in both models, Age and CESAL possess a high correlation with the IRI, while YESAL possesses a moderate correlation with the IRI in the AC model. Although the impact of the CESAL is higher than the YESAL in modeling the IRI_{AC}, the YESAL was used to avoid multicollinearity among Age and CESAL where the moderate correlation (0.62) between them was replaced with the low correlation (0.31) between Age and the YESAL. Since the correlation between Age and CESAL in the DBST model is as low as 0.42, CESAL was used without any multicollinearity concern.

1.2. Artificial neural network models

An ANN is a form of an Artificial Intelligence (AI) applied to resolve nonlinear engineering problems such as estimating current and predicting future pavement conditions (Adeli, 2001). An ANN is a computational intelligence system that mimics the human brain's information processing and knowledge acquisition (Georgiou et al., 2018) and consists of many neurons interconnected through directed links, and each link has an associated weight. The weights acquired through the training process represent abstracted information from the data set, which an ANN uses to solve a particular problem. Three key components need to be determined to construct an ANN: the structure of connection between input and output layers (architecture), the neuron activation function, and the method of adjusting the connection weight (learning method).

1.2.1. Architecture of the ANN

Feedforward Backpropagation ANN is one of the most commonly used neural network that is capable of performing any linear and nonlinear computations and representing any function arbitrarily well (Xu et al., 2014). Feedforward means no lateral connection exists between the artificial neurons in a given layer, and the data flow does not go back to previous layers (Chou & Pellinen, 2005). An ANN is generally constructed from an input layer where there are as many neurons as the independent variables considered in the analysis, one or several hidden layers of neurons, and an output layer with as many neurons as the number of dependent variables.

A network with *n* hidden layers is usually called an "*n* + 1-layer network" as the input layer does not perform any calculations on the data. There is no specific standard procedure to determine the number of hidden layers in a neural network. Researchers usually use trial and error to
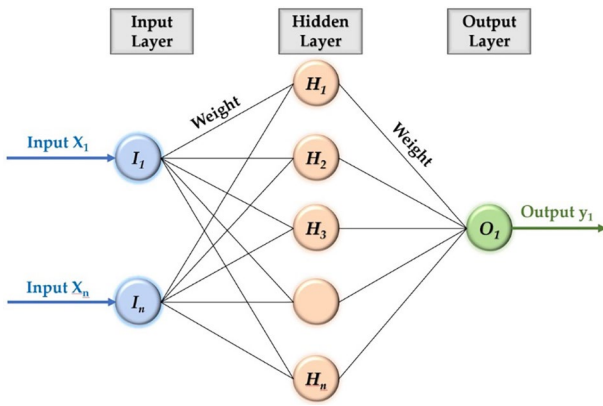
Table 5. Pearson correlation coefficient matrixes

DBST Model				AC Model				
Variable	IRI	AGE	CESAL	Variable	IRI	AGE	CESAL	YEASL
IRI	1	0.85	0.73	IRI	1	0.82	0.83	0.64
AGE	0.85	1	0.42	AGE	0.82	1	0.62	0.31
CESAL	0.73	0.42	1	CESAL	0.83	0.62	1	0.90
				YESAL	0.64	0.31	0.90	1

Figure 4. The general architecture of the feedforward backpropagation ANN

Figure 5. Basic artificial neuron

find the optimum number of hidden layers and neurons in each hidden layer. Figure 4 presents the general architecture of the feedforward backpropagation neural network that is most used.

1.2.2. Activation function

Each neuron in the ANN works as a processing unit, as illustrated in Figure 5, receiving inputs and turn over the output to the next layer (Huang & Moore, 1997). All neurons of a given layer are connected to all neurons in the subsequent layer.

The nonlinear relationship between variables in input and output layers in the ANN needs a function to create a relation between neurons. Computation between two neurons of different layers in the neural network is provided by three transfer functions: Log-Sigmoid, Tan-Sigmoid, and Linear (Demuth & Beale, 1992). These functions have the following mathematical Eqns (3)–(5):

$$\text{logsig}\left(x\right)=\frac{1}{1+e^{-x}}\,; \tag{3}$$

$$\text{tansig}\left(x\right)=\frac{2}{1+e^{-2x}}-1\,; \tag{4}$$

$$\text{purelin}\left(x\right)=x\,. \tag{5}$$

The sigmoid function and linear threshold function were used in this study for the hidden layer and output layer. The processing of each neuron is simply a weighted summation that is transferred via activation function, which is shown as the following Eqn (6) (Mosa, 2017):

$$O_j=f\sum_{i=1}^{n}x_iw_{ij}, \tag{6}$$

where: O_j is the output of jth neuron, f is the activation function, n is the total number of inputs in this layer, X_i is ith input, W_{ij} is the connection weight between ith input and jth neuron.

1.2.3. Learning algorithm

Levenberg-Marquardt's backpropagation (LMBP) algorithm is a numerical optimization technique for training
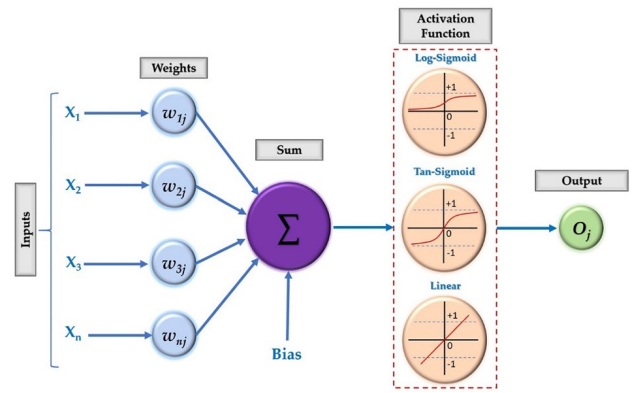
the neural network (Demuth & Beale, 1992). The network will be trained in standard training procedures conducted in three steps. The first step is the feedforward of the input training dataset, where the input data is passed forward through the network to reach the output layer. After that, the associated error at the output layer is calculated. Lastly, the errors are propagated back towards the input layer, where weights and biases of the network are iteratively adjusted to minimize the network performance function. The performance function for feedforward networks is the Mean Square Error (MSE). MSE is the average squared error between the network outputs and the target outputs.

1.3. Models' performance measures

The performance of the developed models will be evaluated in terms of statistical measures of goodness of fit. There are many statistical criteria for evaluating the performance of the developed models. In this research, the proposed models were assessed utilizing the coefficient of determination (R^2), Mean Absolute Error (MAE), and the Root Mean Squared Percentage Error (RMSPE). The corresponding equations are mathematically defined through Eqns (7)–(9) (Hamdi et al., 2017):

$$R^2=1-\frac{\sum_{i=1}^{n}\left(IRI_{i,act}-IRI_{i,pred}\right)^2}{\sum_{i=1}^{n}(IRI_{i,act}-\overline{IRI}_{act})^2}\,; \tag{7}$$

$$\text{MAE}=\frac{1}{n}\sum_{i=1}^{n}\left|IRI_{i,act}-IRI_{i,pred}\right|\,; \tag{8}$$

$$\text{RMSPE}=\sqrt{\frac{1}{n}\sum_{i=1}^{n}\left(\frac{IRI_{i,act}-IRI_{i,pred}}{IRI_{i,act}}\right)^2}\,, \tag{9}$$

where: n is the number of samples, IRI_{act} and IRI_{pred} are the actual and the predicted IRI value, respectively, $\overline{IRI}_{act}$ is the average value of actual IRI.

The R^2 should be close to 1 for a better correlation between the predicted and the actual values, while the lower values of MAE and RMSPE correspond to a higher forecasting capacity and lower error for predicted values.

2. Results

2.1. ANN model development

The current study utilized the same database for the MLR models (Gharieb & Nishikawa, 2021) to develop an ANN model for each type of pavement. Pavement Age and CESAL are used as input variables for predicting the IRI value. Despite the significant influence of the environmental factors, subgrade soil properties, pavement structural capacity, and initial IRI_0 value on the progression of the unevenness (Makendran et al., 2015; Mazari & Rodriguez, 2016; Odoki & Kerali, 2001; Sandra & Sarkar, 2013), an assessment of the effect of those factors on IRI progression was not possible, since the Laos PMS database does not have any information regarding those variables. The obtained data were randomly divided into training (70%), validation (15%), and testing (15%) datasets. The dataset range covers a broad range of pavement conditions under different traffic loading characteristics, raising confidence in the proposed models. Figure 6 shows the histogram and the normal probability distribution of the IRI, Age, CESAL, and YESAL. The figure shows that the distributions of input and output variables are not fully normally distributed and not similar, which means the relationship between the input variables (Age and CESAL or YESAL) and IRI is nonlinear.
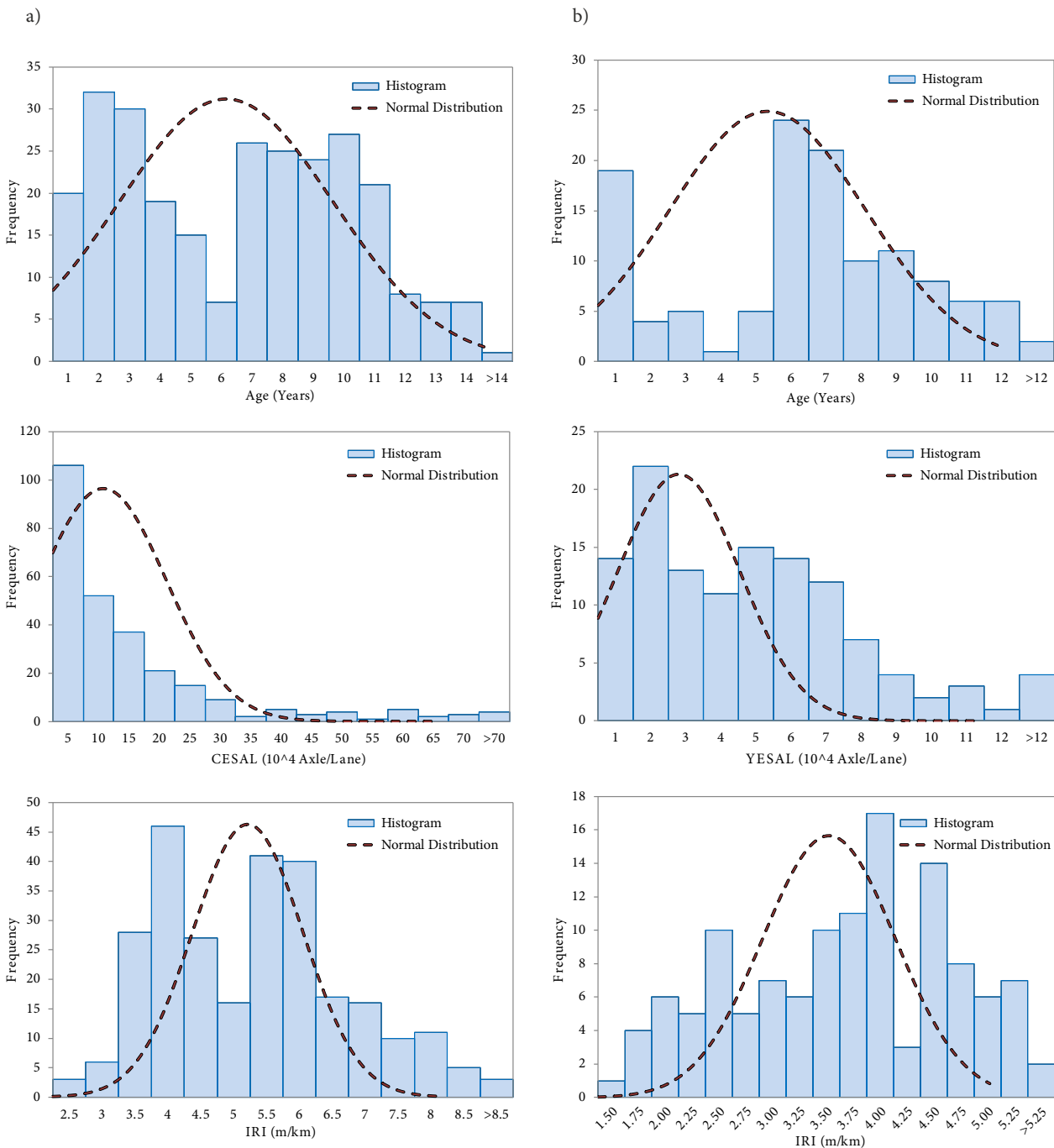
a)

b)

Figure 6. Histogram along with the normal probability distribution for: a – DBST; b – AC models variables

The descriptive statistics of variables used for training, validation, testing, and all datasets in both DBST and AC models are summarized in Table 6. The training data are used to fit the model, while the validation data are used to avoid overfitting. The test data are used to compute the quality of the prediction estimates.

Development of ANN models were conducted using the Neural Network Toolbox incorporated in the MATLAB R2020b. A two-layer feed-forward ANN (excluding the input layer) with a tan-sigmoid transfer function in the hidden layer and a linear transfer function in the output layer was created. The Levenberg-Marquardt backpropagation algorithm was used for training the models.

To form an accurate ANN model, a trial-and-error process could be used to judge the number of neurons in the hidden layer. There is no standard method for selecting the appropriate number of neurons, so training the ANN model with a sequential number of hidden neurons and then selecting the number of neurons that achieve minimum MSE was employed.

As an initial guess, two neurons were used in the hidden layer. Trial networks with a varying number of neurons in the hidden layer were trained to evaluate the performance of different network architectures. Ten trials were conducted for each number of neurons in the hidden layer then the average values were calculated and plotted as shown in Figure 7.

The results indicate that the MSE is sensitive to the number of neurons in the hidden layer, where MSE decreases as the number of neurons in the hidden layer increase. The lowest MSE value was achieved at 9 and 11 hidden neurons for DBST and AC models.

After determining the optimum number of neurons in the hidden layer, Figure 8 displays the architecture of the proposed neural network models for the DBST and the AC pavement sections. DBST neural network architecture is composed of one input layer including two neurons (Age and CESAL), one output layer including one neuron (IRI), and one hidden layer in between with nine neurons (2-9-1). Similar configurations were used for developing ANN for the AC pavement sections, with a different number of neurons in the hidden layer (2-11-1).

The final neural network architecture was retrained several times using the training data set to guarantee that it has the best solution and to find the correct weights for the optimum solution. The connection weights are initially appointed randomly. Figure 9 illustrates the error performance versus epochs to check the progress while training, validating, and testing the ANN. Epochs are the number of learning cycles where weights were adjusted to minimize the difference between the measured and the predicted IRI.

Table 6. Descriptive statistics of the variables used for IRI modeling

| Variable	Training (70%)				Validation (15%)				Test (15%)				All data			
	Min	Max	Mean	Std	Min	Max	Mean	Std	Min	Max	Mean	Std	Min	Max	Mean	Std
DBST Model																
Age	0.01	14.10	6.16	3.70	0.17	13.39	6.13	3.88	0.11	13.39	5.28	3.73	0.10	14.10	6.03	3.73
CESAL	0.02	99.26	13.88	16.63	0.02	64.41	13.40	16.08	0.02	87.07	10.34	16.68	0.02	99.26	13.28	16.55
IRI	2.20	8.91	5.17	1.45	2.46	8.83	5.06	1.50	2.93	8.18	4.73	1.28	2.20	8.91	5.09	1.44
AC Model																
Age	0.09	12.08	5.82	3.45	0.09	13.08	6.73	3.83	0.15	10.76	5.74	3.01	0.09	13.08	5.95	3.44
YESAL	0.03	20.53	4.56	3.61	0.73	10.13	3.99	2.41	0.50	10.32	4.20	2.90	0.03	20.53	4.42	3.34
IRI	1.47	5.46	3.52	1.04	1.63	5.18	3.75	1.06	1.73	4.52	3.41	0.90	1.47	5.46	3.54	1.02

a) DBST model
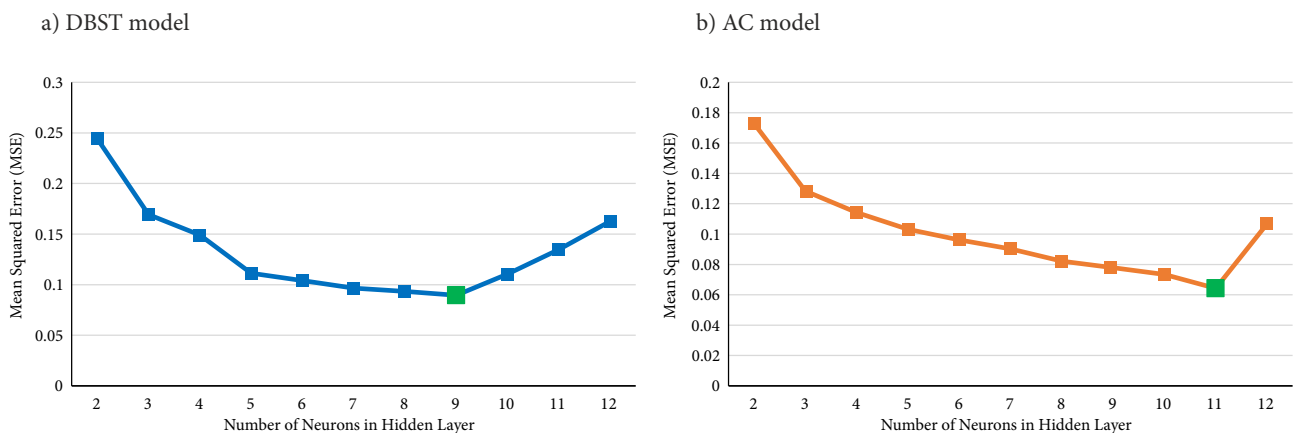
b) AC model

Figure 7. Progress of MSE versus the number of neurons in the hidden layer for the: a – DBST model; b – AC model

a)

b)

Figure 8. Neural network architecture for the:
a – DBST model; b – AC model

a)

b)

Figure 9. ANN Error performance while training, validation,
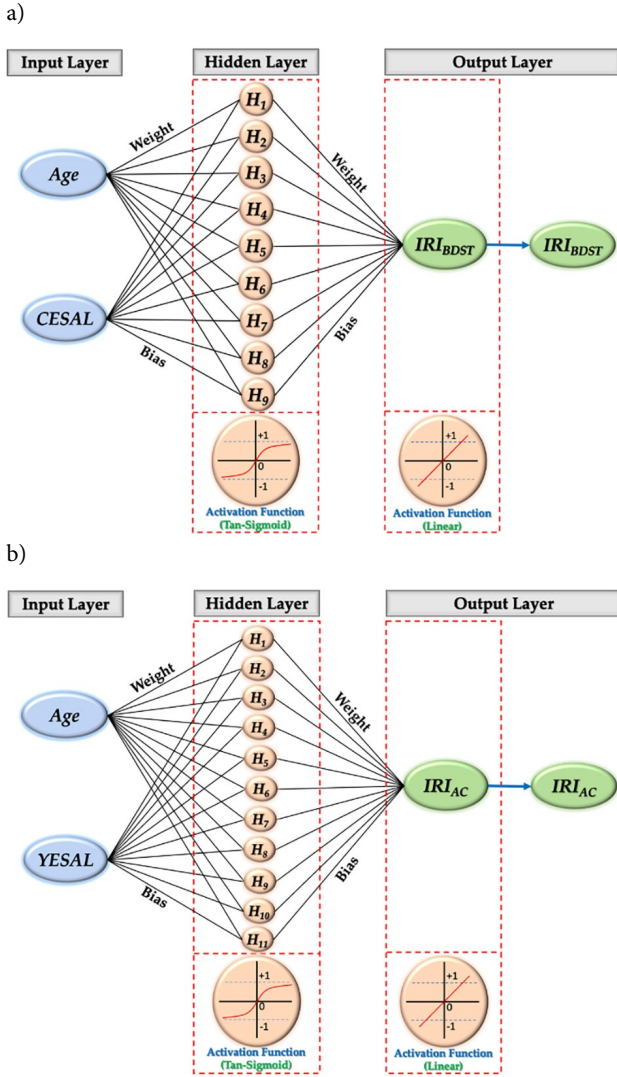and testing for the: a – DBST model; b – AC model

The error function in terms of MSE between the measured and the predicted IRI was monitored during the training process. When the network begins to overfit the data, the error on the validation set will begin to increase, so the training was stopped, and the network weights and biases were maintained at the minimum of the validation set error, as shown in Tables A2, A3, and A4 in Appendix.

The results revealed that the MSE decreases with the training epochs. For DBST pavement sections, the best training performance of the model is gained at epoch 13, where the validation error is equal to 0.099. At the same time, the best training performance of the AC model is achieved at epoch 31, where the validation error is equal to 0.058.

2.2. Models' evaluation

To ensure the good generalization ability of a trained neural network, once each network was developed using a training dataset and validated, it was tested using the test dataset.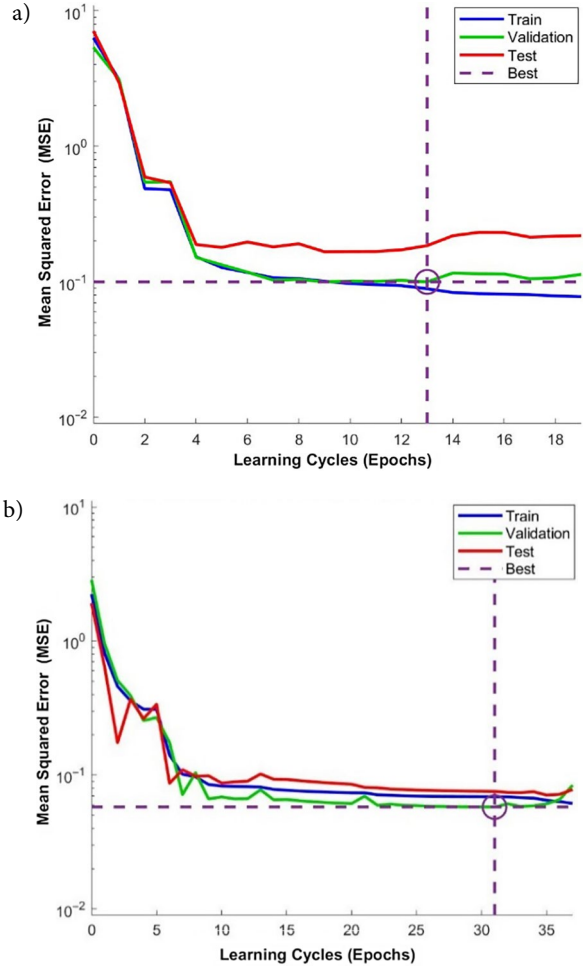 Like the validation dataset, a test dataset is never used for training the neural network. Figures 10 and 11 show scatter plots of the measured and the predicted IRI values of DBST and AC pavement sections, respectively, using the ANN model for training, validation, testing, and all datasets.

The figures showed good distribution of data points around the equality line, indicating a highly accurate prediction of the developed models. The equality line is the target of the training activity. Moreover, the R^2, MAE, and RMSPE were calculated for training, validation, testing, and all datasets in both DBST and AC models as shown in Table 7.

The values of R^2, MSA, and RMSPE for the DBST model were equal to 0.949, 0.244, and 7.331, respectively, whereas they were equal to 0.934, 0.193, and 9.652 for the AC model, considering all dataset. Larger values of R^2 and lower values of MAE/RMSPE suggest that a strong correlation exists between the predicted and the measured IRI values.

In addition, Figure 12 shows the histogram of the prediction errors for training, validation, and testing datasets in both DBST and AC models. The prediction errors are statistically normally distributed. As can be seen in Figure 12a, the prediction errors in the DBST model are
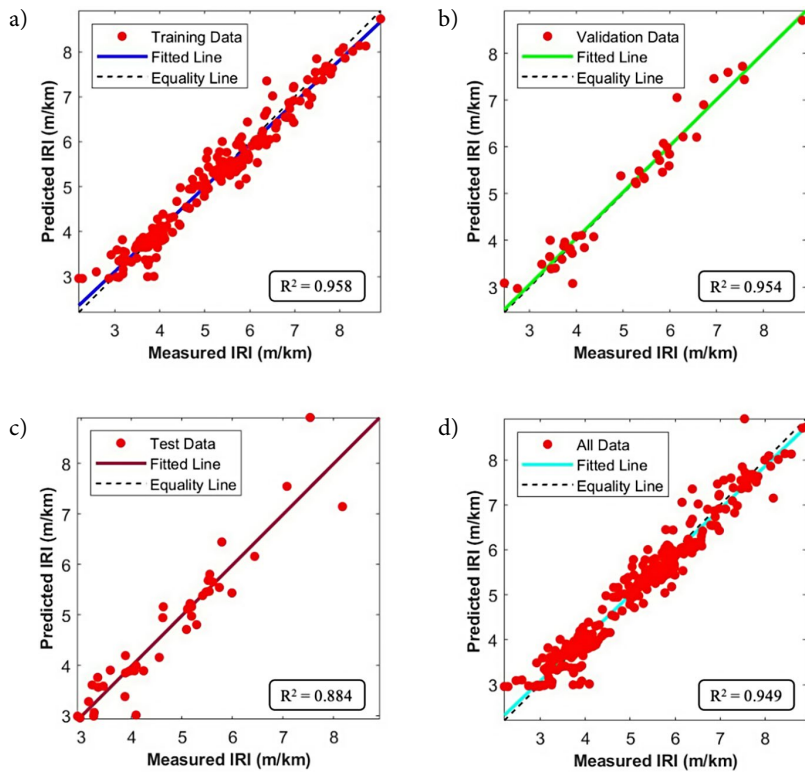
Figure 10. DBST model goodness-of-fit results of the: a – Training data; b – Validation data; c – Test data; d – All data
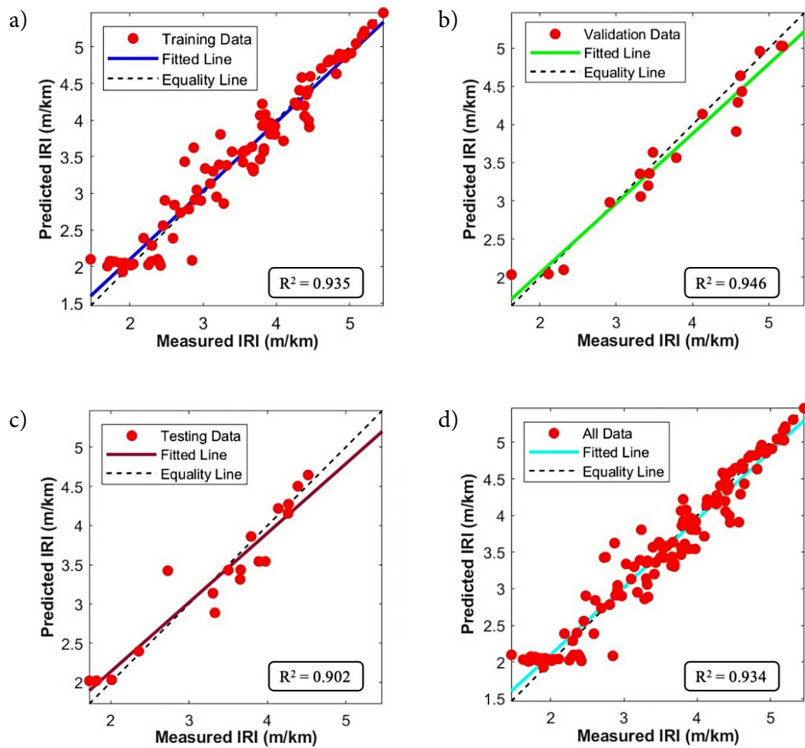

Figure 11. AC model goodness-of-fit results of the: a – Training data; b – Validation data; c – Test data; d – All data

mainly concentrated between –0.70 and 0.53 m/km, while the prediction errors in the AC model are mainly concentrated between –0.41 and 0.42 m/km, as shown in Figure 12b. The results shown in Figure 12 confirm what has illustrated in Table 7 that MAE values in the AC model are less than those in the DBST model. Overall, the statistical evaluation results reveal that both models have good prediction ability and their R^2 values show their success in modeling the IRI.

Table 7. Performance of the DBST and the AC models of training, validation, testing, and all data

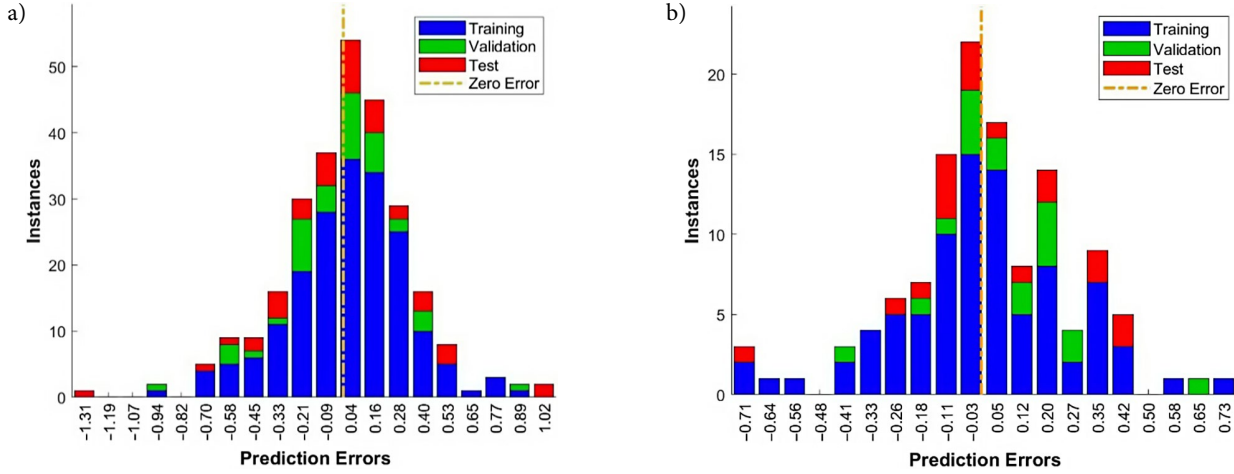| Parameter	DBST model				AC model			
	Training	Validation	Test	All	Training	Validation	Test	All
n	189	40	40	269	86	18	18	122
R^2	0.958	0.954	0.884	0.949	0.935	0.946	0.902	0.934
MAE	0.231	0.237	0.309	0.244	0.191	0.183	0.209	0.193
RMSPE	7.026	7.596	8.394	7.331	9.979	8.123	9.467	9.652

Figure 12. Distribution of the ANN prediction errors for the: a – DBST model; b – AC model

2.3. Sensitivity analysis of the ANN model

The relative importance of each input variable to the IRI prediction was studied employing sensitivity analysis. Two methods can conduct ANN sensitivity analysis; the weights method as firstly proposed by Garson (1991) and the first-order partial derivative method (Nourani & Sayyah Fard, 2012; Shekharan, 1999). In this study, the weight method was employed as it comprises less calculations while gives comparable results to the second method (Liu, 2013). The Weights method is a process of splitting the connection weights (Tables A2 and A3) to determine the relative importance of the different inputs. This method basically involves splitting the hidden-output connection weights of every hidden neuron into components connected with every input neuron, using absolute values of all weights (Goh, 1995). By utilizing Eqn (10) (Jokić et al., 2011), the relative importance of input variables to IRI prediction for DBST and AC pavement sections was computed as a percentage value. For each model, the sum of relative importance values of all input variables must be 100%.

$$R_i = \frac{\sum_{j=1}^{n_h}\left[\left(\dfrac{w_{vj}}{\sum_{k=1}^{n_v} i_{kj}}\right)O_j\right]}{\sum_{i=j}^{n_v}\left[\sum_{j=1}^{n_h}\left[\left(\dfrac{w_{vj}}{\sum_{k=1}^{n_v} i_{kj}}\right)O_j\right]\right]}, \qquad (10)$$

where: R_i is the relative importance of each input variable, n_h is the hidden neurons' number, n_v is the input neurons number, w_j is the input-hidden connection weights, and O_j is the hidden-output connection weights.

The calculated R_i values are within 0 and 1. A larger R_i value points out a greater impact of the corresponding input variable on the predicted IRI. As illustrated in Table 8, the results of sensitivity analysis indicate that, for the DBST model, both age and CESAL play a remarkable role in IRI predictions, as there is no significant difference in the relative importance values between them. While in the AC model, age plays the most crucial role in IRI predictions. The cause of this phenomenon might be due to the effect of pavement structural capacity, where under the same range of traffic loads, AC pavement sections are less affected than DBST pavement sections.

Table 8. The relative importance of ANN input variables

Variables	DBST model		AC model	
	Age	CESAL	Age	YESAL
R_i (%)	46.86	53.14	67.15	32.85

2.4. Comparative study

The proposed ANN models were compared statistically with the previous developed MLR models (Gharieb & Nishikawa, 2021) for both DBST and AC pavement sections. For the first level of comparison, R^2, MAE, and RMSPE were calculated for the ANN and the MLR models using training datasets. From the results reported in Table 9, it

can be observed that the ANN models for both BDST and AC pavement sections present high R^2 and low MAE and RMSPE values, although the goodness-of-fit statistics of the MLR models for both DBST and AC pavement sections are less efficient compared with those corresponding to ANN models.

In the second level of comparison, the ANN model's performance in predicting the IRI values is compared with those produced by the MLR method and the measured values, as shown in Figure 13. The comparison is carried out utilizing validation and testing datasets. Figure 13a shows that both DBST models (ANN and MLR) have almost the same prediction ability with high values of R^2 (0.930 and 0.923) where the two lines (ANN IRI and MLR IRI) are almost parallel to the Measured IRI line with some minor differences. While for AC pavement sections, the ANN model is more precise than the MLR model,

with a much higher R^2 value of 0.935 compared to 0.849 for the MLR model. Also, the results shown in Figure 13b confirm this where the differences between lines ANN IRI and Measured IRI are less than those between lines MLR IRI and Measured IRI.

From those results illustrated in Table 9 and Figure 13, It is noteworthy to mention that both methods have outstanding predictive ability. However, it can be concluded that the proposed ANN models yield superior performance and precise predictions compared to the MLR models using the same database.

Conclusions

ANN can be used in PMS to estimate current and predict future pavement conditions, assess maintenance needs, and select maintenance and rehabilitation strategies. Laos' road maintenance strategy is mainly based on assessing pavement roughness in terms of the IRI. Laos PMS uses default HDM-4 pavement deterioration models without calibration to predict the IRI, which leads to an enormous error between measured and predicted IRI values.

Thus, a typical three-layer feedforward backpropagation ANN was applied in this research to develop new IRI prediction models for two families of pavement: DBST and AC, to operate PMS properly. Models' variables were extracted from the Laos PMS database. The Levenberg Marquardt algorithm was employed for training.

Table 9. Comparison of the goodness of fit statistics for the ANN and the MLR models

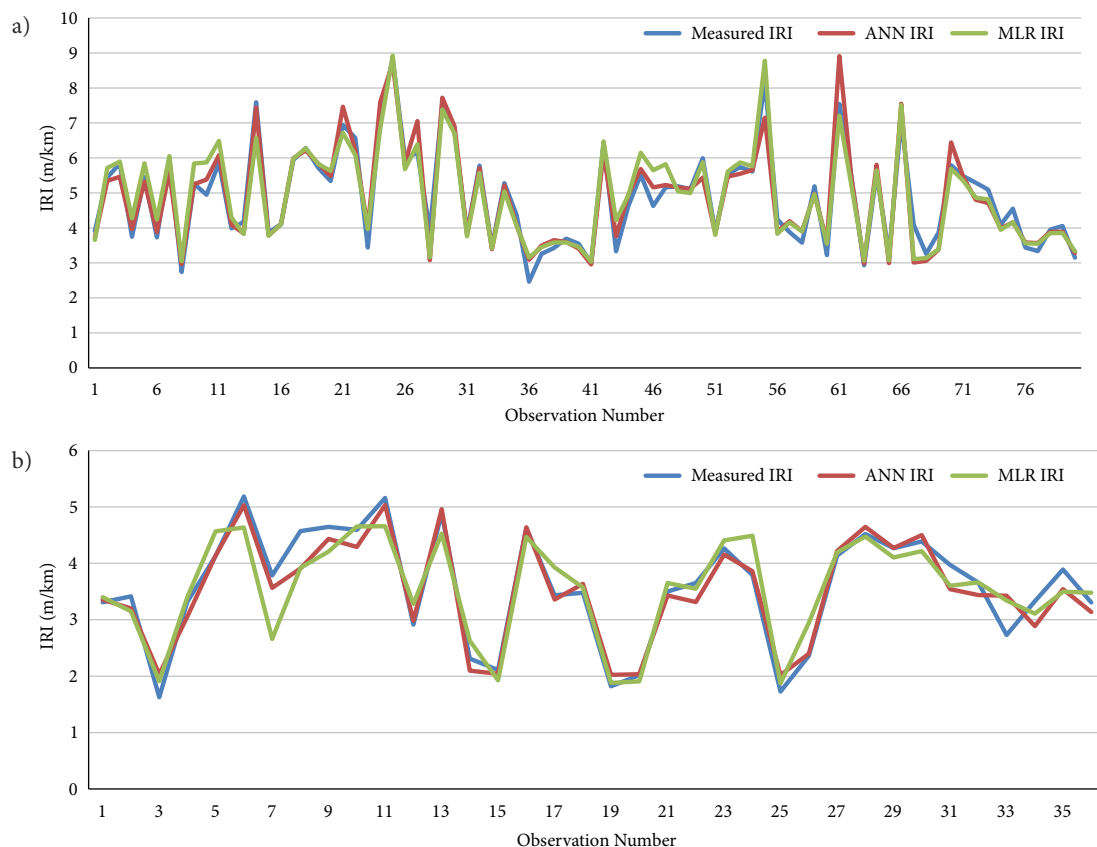| Parameter	DBST Model		AC Model	
	ANN	MLR	ANN	MLR
n	189	215	86	98
R^2	0.958	0.892	0.935	0.847
MAE	0.231	0.336	0.191	0.314
RMSPE	7.026	9.626	9.979	12.186

Figure 13. Comparing the measured IRI with the predicted IRI calculated by the MLR and the ANN models for the:
a – DBST pavement sections; b – AC pavement sections

The developed ANN models successfully predicted the IRI with R^2 values of 0.96 and 0.94 for the training dataset of DBST and AC models, respectively. The performance of the proposed ANN models is deemed much better compared to the similar MLR models developed previously.

Despite the better prediction of ANN models' to IRI values, ANN models cannot be incorporated in Laos PMS due to the difficulty of deriving a formula that works with all possible inputs' values. Even if deriving a formula, the developed formula will end up with a long equation including the inputs, weights, and biases which is useless. All these difficulties give an advantage to the MLR models in terms of ease of integrating them into the current system. The effect of the environmental factors, subgrade soil properties, pavement structural capacity, and initial IRI_0 value on the progression of the unevenness will be studied in the future.

Acknowledgements

Funding

Author contributions

The Authors MG and TN conceived the study and were responsible for data collection and analysis. All authors (MG, TN, SN, and KT) were responsible for data interpretation. MG wrote the first draft of the article. Authors (TN, SN, and KT) critically revised the manuscript.

Disclosure statement

Authors confirm that they do not have any competing financial, professional, or personal interests from other parties.

References

American Association of State Highway and Transportation Officials. (2012). *Pavement management guide* (2nd ed.). USA.

Abaza, K. A. (2016). Back-calculation of transition probabilities for Markovian-based pavement performance prediction models. *International Journal of Pavement Engineering*, 17, 253–264. https://doi.org/10.1080/10298436.2014.993185

Abaza, K. A. (2018). Empirical-Markovian model for predicting the overlay design thickness for asphalt concrete pavement. *Road Materials and Pavement Design*, 19, 1617–1635. https://doi.org/10.1080/14680629.2017.1338188

Abd El-Hakim, R., & El-Badawy, S. (2013). International roughness index prediction for rigid pavements: an artificial neural network application. *Advanced Materials Research*, 723, 854–860. https://doi.org/10.4028/www.scientific.net/AMR.723.854

Abdelaziz, N., Abd El-Hakim, R. T., El-Badawy, S. M., & Afify, H. A. (2020). International roughness index prediction model for flexible pavements. *International Journal of Pavement Engineering*, 21, 88–99. https://doi.org/10.1080/10298436.2018.1441414

Abulizi, N., Kawamura, A., Tomiyama, K., & Fujita, S. (2016). Measuring and evaluating of road roughness conditions with a compact road profiler and ArcGIS. *Journal of Traffic and Transportation Engineering* (English Edition), 3, 398–411. https://doi.org/10.1016/j.jtte.2016.09.004

Adeli, H. (2001). Neural networks in civil engineering: 1989–2000. *Computer-Aided Civil and Infrastructure Engineering*, 16, 126–142. https://doi.org/10.1111/0885-9507.00219

Al-Mansour, A. I., & Al-Swailem, S. S. (1999). Pavement condition data collection and evaluation of Riyadh Main Street network. *Journal of King Saud University - Engineering Sciences*, 11(1), 1–17. https://doi.org/10.1016/S1018-3639(18)30987-5

Albuquerque, F. S., & Núñez, W. P. (2011). Development of roughness prediction models for low-volume road networks in northeast Brazil. *Transportation Research Record: Journal of the Transportation Research Board*, 2205, 198–205. https://doi.org/10.3141/2205-25

Alin, A. (2010). Multicollinearity. *Wiley Interdisciplinary Reviews: Computational Statistics*, 2, 370–374. https://doi.org/10.1002/wics.84

ARA. (2001). *Guide for mechanistic-empirical design of new and rehabilitated pavement structures. Appendix OO-1: Background and preliminary smoothness prediction models for flexible pavements*. National Cooperative Highway Research Program.

Asakawa, H., Nagayama, T., Fujino, Y., Nishikawa, T., Akimoto, T., & Izumi, K. (2012). Development of a simple pavement diagnostic system using dynamic responses of an ordinary vehicle. *Journal of Japan Society of Civil Engineers, Ser. E1* (*Pavement Engineering*), 68, 20–31. https://doi.org/10.2208/jscejpe.68.20

Asian Infrastructure Investment Bank. (2009). *Lao People's Democratic Republic: National Road 13 improvement and maintenance project* (PD000066-LAO).

Choi, J. H., Adams, T. M., & Bahia, H. U. (2004). Pavement roughness modeling using back-propagation neural networks. *Computer-Aided Civil and Infrastructure Engineering*, 19, 295–303. https://doi.org/10.1111/j.1467-8667.2004.00356.x

Chou, S. F., & Pellinen, T. K. (2005). Assessment of construction smoothness specification pay factor limits using artificial neural network modeling. *Journal of Transportation Engineering*, 131, 563–570. https://doi.org/10.1061/(ASCE)0733-947X(2005)131:7(563)

Demuth, H., & Beale, M. (1992). *Neural network toolbox for use with MATLAB: User's guide*. Mathworks, Natick, Mass.

Douangphachanh, V., & Oneyama, H. (2014). A study on the use of smartphones under realistic settings to estimate road roughness condition. *EURASIP Journal on Wireless Communications and Networking*, 2014, 114. https://doi.org/10.1186/1687-1499-2014-114

Fujino, Y., Kitagawa, K., Furukawa, T., & Ishii, H. (2005). Development of vehicle intelligent monitoring system (VIMS). In *Proceedings of Smart Structures and Materials 2005: Sensors and Smart Structures Technologies for Civil, Mechanical, and Aerospace Systems* (Vol. 5765). https://doi.org/10.1117/12.601727

Garson, D. G. (1991). Interpreting neural network connection weights. *AI Expert*, 6(4), 46–51.

George, K. P., Rajagopal, A .S., & Lim, L. K. (1989). Models for predicting pavement deterioration. *Transportation Research Record*, 1215.

Georgiou, P., Plati, C., & Loizos, A. (2018). Soft computing models to predict pavement roughness: A comparative study. *Advances in Civil Engineering*, 2018, 5939806. https://doi.org/10.1155/2018/5939806

Gharieb, M., & Nishikawa, T. (2021). Development of roughness prediction models for Laos national road network. *CivilEng*, 2, 158–173. https://doi.org/10.3390/civileng2010009

Goh, A. T. C. (1995). Back-propagation neural networks for modeling complex systems. *Artificial Intelligence in Engineering*, 9, 143–151. https://doi.org/10.1016/0954-1810(94)00011-S

Gupta, A., Kumar, P., & Rastogi, R. (2011). Pavement deterioration and maintenance model for low volume roads. *International Journal of Pavement Research and Technology*, 4, 195–202. https://doi.org/10.6135/ijprt.org.tw/2011.4(4).195

Hamdi, Hadiwardoyo, S. P., Correia, A. G., Pereira, P., & Cortez, P. (2017). Prediction of surface distress using neural networks. *AIP Conference Proceedings*, 1855, 040006. https://doi.org/10.1063/1.4985502

Hossain, M., Gopisetti, L. S. P., & Miah, M. S. (2020). Artificial neural network modelling to predict international roughness index of rigid pavements. *International Journal of Pavement Research and Technology*, 13, 229–239. https://doi.org/10.1007/s42947-020-0178-x

Huang, Y., & Moore, R. K. (1997). Roughness level probability prediction using artificial neural networks. *Transportation Research Record: Journal of the Transportation Research Board*, 1592, 89–97. https://doi.org/10.3141/1592-11

Japan International Cooperation Agency (JICA), & Mitsubishi Research Institute (2013). *Information collection and confirmation survey on road and bridge maintenance management* (Final report, Summary).

Jokić, A., Grahovac, J., Dodić, J., Dodić, S., Popov, S., & Vucurovic, D. (2011). Interpreting the neural networkfor prediction of fermentation of thick juice from sugar beet processing. *Acta Periodica Technologica*, 42, 241–249. https://doi.org/10.2298/APT1142241J

Justo-Silva, R., Ferreira, A., & Flintsch, G. (2021). Review on machine learning techniques for developing pavement performance prediction models. *Sustainability*, 13, 5248. https://doi.org/10.3390/su13095248

Kaloop, M., El-Badawy, S., Ahn, J., Sim, H.-B., Hu, J., & Abd El-Hakim, R. (2020). A hybrid wavelet-optimally-pruned extreme learning machine model for the estimation of International Roughness Index of rigid pavements. *International Journal of Pavement Engineering*. https://doi.org/10.1080/10298436.2020.1776281

Kırbaş, U., & Karaşahin, M. (2016). Performance models for hot mix asphalt pavements in urban roads. *Construction and Building Materials*, 116, 281–288. https://doi.org/10.1016/j.conbuildmat.2016.04.118

La Torre, F., Domenichini, L., & Darter, M. I. (1998). Roughness prediction model based on the artificial neural network approach. In *Fourth International Conference on Managing Pavements*.

Laos Ministry of Public Works and Transport. (2020). *Summary of road network statistics year*. Laos.

Laos Ministry of Public Works and Transport. (2018). *Road design manual*. Laos.

Lin, J.-D., Yau, J.-T., & Hsiao, L.-H. (2003). Correlation analysis between international roughness index (IRI) and pavement distress by neural network. In *82nd Annual Meeting of the Transportation Research Board* (pp. 12–16), Transportation Research Board, Washington, D.C.

Liu, L. (2013). *A methodology for developing performance-related specifications for pavement preservation treatments* [Dissertation]. Texas A&M University, Texas, USA.

Makendran, C., Murugasan, R., & Velmurugan, S. (2015). Performance prediction modelling for flexible pavement on low volume roads using multiple linear regression analysis. *Journal of Applied Mathematics*, 2015, 192485. https://doi.org/10.1155/2015/192485

Mazari, M., & Rodriguez, D. D. (2016). Prediction of pavement roughness using a hybrid gene expression programming-neural network technique. *Journal of Traffic and Transportation Engineering* (English Edition), 3, 448–455. https://doi.org/10.1016/j.jtte.2016.09.007

Mosa, A. M. (2017). Neural network for flexible pavement maintenance and rehabilitation. *Applied Research Journal*, 3, 114–129.

Múčka, P. (2017). International Roughness Index specifications around the world. *Road Materials and Pavement Design*, 18, 929–965. https://doi.org/10.1080/14680629.2016.1197144

Nguyen, H.-L., Pham, B. T., Son, L. H., Thang, N. T., Ly, H.-B., Le, T.-T., Ho, L. S., Le, T.-H., & Tien Bui, D. (2019). Adaptive network based fuzzy inference system with meta-heuristic optimizations for international roughness index prediction. *Applied Sciences*, 9, 4715. https://doi.org/10.3390/app9214715

Nourani, V., & Sayyah Fard, M. (2012). Sensitivity analysis of the artificial neural network outputs in simulation of the evaporation process at different climatologic regimes. *Advances in Engineering Software*, 47, 127–146. https://doi.org/10.1016/j.advengsoft.2011.12.014

Obunguta, F., & Matsushima, K. (2020). Optimal pavement management strategy development with a stochastic model and its practical application to Ugandan national roads. *International Journal of Pavement Engineering*. https://doi.org/10.1080/10298436.2020.1857759

Odoki, J. B., & Kerali, G. R. H. (2001). *Volume four: Analytical framework and model descriptions. Highway Development and Management Model HDM-4* (*Version 1.2*). World Road Association.

Olowosulu, A. T., Kaura, J. M., Murana, A. A., & Adeke, P. T. (2021). Development of framework for performance prediction of flexible road pavement in Nigeria using Fuzzy logic theory. *International Journal of Pavement Engineering*. https://doi.org/10.1080/10298436.2021.1922907

Owusu-Ababio, S. (2002). Effect of neural network topology on flexible pavement cracking prediction. *Computer-Aided Civil and Infrastructure Engineering*, 13, 349–355. https://doi.org/10.1111/0885-9507.00113

Pérez-Acebo, H., Gonzalo-Orden, H., Findley, D. J., & Rojí, E. (2021). Modeling the international roughness index performance on semi-rigid pavements in single carriageway roads. *Construction and Building Materials*, 272, 121665. https://doi.org/10.1016/j.conbuildmat.2020.121665

Pérez-Acebo, H., Linares-Unamunzaga, A., Rojí, E., & Gonzalo-Orden, H. (2020). IRI performance models for flexible pavements in two-lane roads until first maintenance and/or rehabilitation work. *Coatings*, 10(2), 97. https://doi.org/10.3390/coatings10020097

Pérez-Acebo, H., Mindra, N., Railean, A., & Rojí, E. (2019). Rigid pavement performance models by means of Markov Chains with half-year step time. *International Journal of Pavement Engineering*, 20, 830–843. https://doi.org/10.1080/10298436.2017.1353390

Sandra, A. K., & Sarkar, A. K. (2013). Development of a model for estimating International Roughness Index from pavement distresses. *International Journal of Pavement Engineering*, 14, 715–724. https://doi.org/10.1080/10298436.2012.703322

Sayers, M. W., Gillespie, T. D., & Queiroz, C. A. V. (1986a). *International experiment to establish correlations and standard calibration methods for road roughness measurements* (Technical paper number 45). The World Bank, Washington, DC, USA.

Sayers, W. M., Gillespie, T. D., & Paterson, W. D. O. (1986b). *Guidelines for conducting and calibrating road roughness measurements* (Technical paper number 45). The World Bank, Washington, DC, USA.

Shahnazari, H., Tutunchian, M. A., Mashayekhi, M., & Amini, A. A. (2012). Application of soft computing for prediction of pavement condition index. *Journal of Transportation Engineering*, 138, 1495–1506. https://doi.org/10.1061/(ASCE)TE.1943-5436.0000454

Shekharan, A. R. (1999). Assessment of relative contribution of input variables to pavement performance prediction by artificial neural networks. *Transportation Research Record: Journal of the Transportation Research Board*, 1655, 35–41. https://doi.org/10.3141/1655-06

Sidess, A., Ravina, A., & Oged, E. (2020). A model for predicting the deterioration of the international roughness index. *International Journal of Pavement Engineering*. https://doi.org/10.1080/10298436.2020.1804062

Smith, K., & Ram, P. (2016). *Measures and specifying pavement smoothness*. FHWA, Washington, DC, USA.

Sollazzo, G., Fwa, T. F., & Bosurgi, G. (2017). An ANN model to correlate roughness and structural performance in asphalt pavements. *Construction and Building Materials*, 134, 684–693. https://doi.org/10.1016/j.conbuildmat.2016.12.186

Surendrakumar, K., Prashant, N.,& Mayuresh, P. (2013). Application of Markovian probabilistic process to develop a decision support system for pavement maintenance management. *International Journal of Scientific & Technology Research*, 2, 295–303.

Teomete, E., Bayrak, M. B., & Agarwal, M. (2004). Use of artificial neural networks for predicting rigid pavement roughness. In *2004 Transportation Scholars Conference*, Iowa State University, Ames, USA.

Terzi, S. (2013). Modeling for pavement roughness using the ANFIS approach. *Advances in Engineering Software*, 57, 59–64. https://doi.org/https://doi.org/10.1016/j.advengsoft.2012.11.013

Uddin, W. (2006). Pavement management systems. In T. F. Fwa (Ed.), *The handbook of highway engineering*. Taylor & Francis.

Xu, G., Bai, L., & Sun, Z. (2014). Pavement deterioration modeling and prediction for Kentucky interstate and highways. In *Proceedings of the 2014 Industrial and Systems Engineering Research Conference* (pp. 993–1002).

Yamany, M. S., & Abraham, D. M. (2021). Hybrid approach to incorporate preventive maintenance effectiveness into probabilistic pavement performance models. *Journal of Transportation Engineering, Part B: Pavements*, 147, 4020077. https://doi.org/10.1061/JPEODX.0000227

Yamany, M. S., Abraham, D. M., & Labi, S. (2021). Comparative analysis of Markovian methodologies for modeling infrastructure system performance. *Journal of Infrastructure Systems*, 27, 4021003. https://doi.org/10.1061/(ASCE)IS.1943-555X.0000604

Zang, K., Shen, J., Huang, H., Wan, M., & Shi, J. (2018). Assessing and mapping of road surface roughness based on GPS and accelerometer sensors on bicycle-mounted smartphones. *Sensors*, 18, 914. https://doi.org/10.3390/s18030914

Ziari, H., Sobhani, J., Ayoubinejad, J., & Hartmann, T. (2015). Prediction of IRI in short and long terms for flexible pavements: ANN and GMDH methods. *International Journal of Pavement Engineering*, 17, 776–788. https://doi.org/10.1080/10298436.2015.1019498

APPENDIX

Table A1 illustrates the abbreviations and definitions of variables that have been used in the IRI literature review models. Table A2 and Table A3 illustrate the weight matrix for calculating the relative contribution of each input variable in predicting IRI for DBST and AC pavement sections, respectively. As well as, Table A4 illustrates the bias values for hidden and output neurons in DBST and AC ANN models.

Table A1. The abbreviation and definition of variables used in the IRI literature review models

Abbreviation Symbols	Variable Name	Abbreviation Symbols	Variable Name
IRI_0	Initial IRI	RL	Road Level
AGE_0	Initial age	CR	Cracking
AGE	Pavement age since last overlay	AC	Alligator Cracking
ESAL	Equivalent Single-Axle Load	FC	Fatigue Cracking
CESAL	Cumulative ESAL	TCLS	Transverse Cracks Low Severity
AADT	Average Annual Daily Traffic	TCMS	Transverse Cracks Medium Severity
AADTT	Average Annual Daily Truck Traffic	TCHS	Transverse Cracks High Severity
AP	Annual Precipitation	D/P	Digging / Patching
AAP	Annual Average Precipitation	P	Patching
FI	Freezing Index	RUT	Rutting

Abbreviation Symbols	Variable Name	Abbreviation Symbols	Variable Name
AAFI	Annual Average Freezing Index	LRUT	Left Rutting
F/T	Number of Freeze/Thaw Cycles	RRUT	Right Rutting
AAT	Annual Average Temperature	SDRUT	Standard Deviation of Rut Depth
ASC	Asphalt Content	SPALL	Percentage of Joints with Spalling
ACTH	Asphalt Concrete thickness	BLD	Bleeding
STH	Surface Thickness	COR	Corrugation
PTH	Pavement Thickness	STR	Stripping
UTH	Unbound Layer Thickness	TFAULT	Total Joint Faulting
P_{200}	Percent Passing No. 200 sieve	PH	Potholes
SN	Structural Number	MPH	Mild Potholes
UEM	Unbound Layer Elastic Modulus	SPH	Severe Potholes
SEM	Subgrade Elastic Modulus	MMH	Mild Manholes
ACEM	Asphalt Concrete Elastic Modulus	SMH	Severe Manholes
AAMiH	Annual Average Minimum Humidity	AAMaH	Annual Average Maximum Humidity
R.Age	The real age of the pavement	SURF	The bituminous material of the surface layer
TotVeh	The accumulated vehicles that circulated through the section in both direction	BASE	The coefficient that considers the combination of material to create a semi-rigid pavement
TotH.Veh	The accumulated number of heavy vehicles that crossed the section in the design lane	Bthick	The thickness of the treated base layer
TotBit	The total thickness of the bituminous layers	GMDH	Group Method of Data Handling
WOPELM	Wavelet Optimally Pruned Extreme Learning Machine	GANFIS	Genetic Algorithm based Adaptive Network-Based Fuzzy Inference System
PSOANFIS	Particle Swarm Optimization based Adaptive Network-Based Fuzzy Inference System	FAANFIS	Firefly Algorithm based Adaptive Network-Based Fuzzy Inference System
SVM	Support Vector Machine	ANFIS	Adaptive Neural-Based Fuzzy Inference System

Table A2. The weight matrix of variables used in DBST ANN model

Variable	H1	H2	H3	H4	H5	H6	H7	H8	H9
Age	1.96	−0.94	−6.22	−8.54	3.60	−6.58	−5.48	0.15	−3.20
CESAL	3.20	4.53	6.63	−0.43	3.28	−3.61	1.28	3.95	2.53
IRIpred	−0.17	0.14	0.10	−0.22	0.17	−0.24	−0.12	0.35	−0.08

Table A3. The weight matrix of variables used in AC ANN model

Variable	H1	H2	H3	H4	H5	H6	H7	H8	H9	H10	H11
Age	−7.70	4.20	3.63	3.40	−6.50	−1.18	−6.97	1.39	−18.14	−2.74	2.25
YESAL	0.25	−6.37	−1.21	−0.45	4.45	−6.35	0.14	9.96	2.76	3.80	1.72
IRIpred	−0.27	−0.61	−3.07	3.58	0.55	0.99	−0.42	0.69	−0.48	0.49	0.71

Table A4. The Bias matrix of variables

Model	H1	H2	H3	H4	H5	H6	H7	H8	H9	H10	H11	Out layer
DBST	−4.77	−2.16	3.82	5.74	0.56	−5.00	−2.66	4.29	−4.47	–	–	−0.31
AC	5.76	−7.70	−1.93	−1.44	0.21	−2.39	−1.42	4.09	−10.09	−4.31	5.47	−0.64